

## Measuring the relative humidity within an error of 0.1% by Arduino

MATSUO, Ryo<sup>1\*</sup> ; SAKAI, Satoshi<sup>1</sup>

<sup>1</sup>Graduate School of Human and Environmental Studies, Kyoto University

It is said that the forest is cooler than the city. We measure the temperature and relative humidity at Kyoto University and Mt.Yoshida to find what causes the difference.

We used humidity and temperature sensor IC within an error of 0.1 percent.

We found that always forest is cooler and wetter than city. However the latent heat of vaporization of water did not cool the air on a day change.

Keywords: relative humidity, tempature, measure, Arduino, Forest and City

## Spontaneous rotation of a block of ice on a flat surface of a warm metal column

TANAKA, Masashi<sup>1\*</sup> ; HOHOKABE, Hirotaka<sup>1</sup> ; YOSHIDA, Shigeo<sup>2</sup> ; NAKAJIMA, Kensuke<sup>2</sup>

<sup>1</sup>Graduate School of Science, Kyushu University, <sup>2</sup>Faculty of Science, Kyushu University

### Summary

We have discovered that a block of ice placed on a flat surface of a warm brass column rotates slowly without any external mechanical driving force.

### Description of the Phenomenon

A column of brass, whose radius and height are 8cm and 16cm, respectively, is placed with its flat surface set horizontally. After it is warmed at least to the room temperature, a flat bottomed block of home-made ice, whose radius and height are 10cm and 4cm, respectively, is placed on the flat surface of the brass column. As the block of ice melts, it begins to rotate about the vertical axis spontaneously. The direction of the rotation does not change by itself. However, it reverses instantaneously if we gently tap the ice block to the opposite direction. The rotation period is typically about 20 seconds. The rotation stops when the brass column cools or when the ice block melts and the brass surface becomes exposed.

### The Importance of Bubbles between the Ice and the Brass Surface

If we use a block of factory-made ice which contains no bubbles, the ice does not rotate. However, if we drill non-through holes on the bottom surface of the ice block so that air bubbles shall be supplied between the ice and brass surface as the ice block melts, the ice rotates. The behavior of the air bubbles observed when the ice rotates and that observed when the ice rotation is blocked are quite different. When the ice rotates, the air bubbles tend to elongate radially and are nearly stationary relative to the brass surface. When the ice is anchored and does not rotate, the air bubbles flow outward, deforming and moving randomly. The observed behaviors above imply a crucial role played by the bubbles in the physics of this phenomenon.

### The Importance of Heat Supply

We measured temperature distribution within the brass column, and found a strong positive correlation between the vertical temperature difference in the column and the angular velocity of the ice rotation. We also conducted a similar experiment using a column of stainless steel, whose thermal conductivity is considerably smaller than brass, the rotation period tends to be quite longer. These observations imply that the flux of heat supplied by the heat conduction in the column of metal is crucial to the emergence of the phenomenon.

### Future Directions

Presently, we have no concrete idea on the dynamics of the phenomenon, even though the strong relationship between the heat supply and the angular velocity suggests that the phenomenon may be interpreted as a kind of heat engine. In the near future, we will conduct more experiments with parameters being better controlled, and with the results of such additional experiments, we will investigate physics of the phenomenon from various aspects.

Keywords: bubble, ice, rotation, heat engine, phase change, spontaneous motion

## Regimes of solutions of an axisymmetric flow in a cylindrical tank with a rotating bottom

IGA, Keita<sup>1\*</sup>

<sup>1</sup>AORI, The University of Tokyo

Non-axisymmetric flows are often observed even in axisymmetric environments in the terrestrial and planetary atmospheres. Such a non-axisymmetry is realized in a simple laboratory experiment using a cylindrical container which is filled with water driven by a rapidly-rotating disk at the bottom. We have been reported on the results of the experiments. When we investigate the mechanism of these phenomena, the solution of the axisymmetric flow realized under this condition is necessary, and we reported last year the expression of the analytical solution obtained using boundary layer theories.

We investigated the features of this analytical solution precisely and extracted some features related to its stability. Applying the solution to the situation with water free surface, we can classify the realized axisymmetric flow into three regimes: (i) Cases where all part of the bottom disk is covered with water and it is divided into inner rigid-body rotation region and outer region with constant angular momentum (ii) Cases where the water exposes the center part of the bottom disk air and the water is divided into inner rigid-body rotation region and outer region with constant angular momentum, and (iii) Cases where the water exposes the center part of the bottom disk air and all the water keeps constant angular momentum. Applying the analytical solution, we elucidated the parameter dependence of the transition between these regimes. Each regime has different characteristic waves, which affects crucially the stability of the flow.

Moreover, in the boundary layer along the side wall, transverse velocity distribution has a jet like structure, which forms negative vorticity gradient region. It is also an important factor which may cause critical layer instability.

Keywords: rotating flow, symmetry breaking, boundary layer, axisymmetric flow, stability

## Benchmark experiments for Venus AGCM: sensitivities to model and astronomical parameters

YAMAMOTO, Masaru<sup>1\*</sup> ; TAKAHASHI, Masaaki<sup>2</sup>

<sup>1</sup>Kyushu University, <sup>2</sup>University of Tokyo

Benchmark experiments and inter-comparisons of atmospheric general circulation models (AGCMs) have been conducted in the climate and Geophysical Fluid Dynamics (GFD) communities. Recently, the AGCM inter-comparisons are extended to Venus and hot extrasolar planets. The ISSI inter-comparison project of Venus AGCM (Lebonnois et al. 2013) shows that there are large differences among the models under the same Venus-like condition, and some model parameters influence the general circulation structures. At the present stage, in the inter-comparisons project, the wave analyses have yet to be fully conducted. For Venus' atmospheric modeling, we need to investigate sensitivity to model parameter (such as resolution), in order to understand the numerical properties of the AGCM and to confirm the model results. In terms of GFD, sensitivity to astronomical parameter (such as planetary rotation) is interesting in profoundly understanding the dynamics of superrotation in a mimic slowly rotating planet, which is represented by the base simulation in the inter-comparison. By using the widely-used benchmark, we can easily compare with previous models. In the present study, the base simulation of the ISSI project is applied to a MIROC AGCM for checking the validity of the Venus model, and is extend to the sensitivity experiments for model resolution (T21, T42, T63, and T106) and planetary rotation (Venus, Titan, and Earth), in which the general circulations and waves are analyzed. In the Venus case, as the model resolution is increased, the total angular momentum of the whole atmosphere becomes larger, although the cloud-top superrotation weakens. This indicates that the high-resolution contributes to the accumulation of the angular momentum in the lower atmosphere. The eddy momentum and heat fluxes in the lower atmosphere are also sensitive to the horizontal resolution. Associated with the eddy heat flux, the indirect circulation is also influenced by the resolution. In T42 and higher resolution experiments, the high-latitude jet and polar indirect circulation are extended to the lower atmosphere. The lower-atmospheric high-latitude jet induces large equatorward eddy angular momentum fluxes. In this presentation, we discuss the sensitivities to model resolution and planetary rotation, based on the transformed Euler mean and Eliassen-Palm flux analyses, which are useful even for slowly rotating planet with very small Coriolis force (although they are not widely used in atmospheric researches of Venus).

## Relationship between structure and replacement of concentric eyewalls in idealized tropical cyclones

TSUJINO, Satoki<sup>1\*</sup> ; TSUBOKI, Kazuhisa<sup>1</sup>

<sup>1</sup>HyARC, Nagoya University

Eyewall is a ring of convective clouds that encircles the eye of a tropical cyclone (TC) such as typhoon and hurricane. TC occasionally has some eyewalls which are called as concentric eyewalls. Once concentric eyewalls are formed, eyewall replacement often occurs. The eyewall replacement is a process that the inner eyewall gradually decays and the outer eyewall moves into the position of the inner (old) eyewall. The wind speed of TC rapidly varies during the replacement (Willoughby, 1987). However, the eyewall replacement does not always occur even if concentric eyewalls are formed and the process of eyewall replacement is not fully known. Tsujino and Tsuboki (2013; the Fall Meeting of the Meteorological Society of Japan) indicated that, on the basis of some analyses of Typhoon Bolaven (2012), the vertical flow of the outer eyewall is weaker than that of the inner eyewall and the outer eyewall tilts relative to the inner eyewall in the long-lived concentric eyewalls. Therefore, we suspect that the eyewall replacement is related to the structure of the concentric eyewalls of TC.

In this study, we investigate the relationship between structure and replacement of concentric eyewalls in some idealized TCs. We conduct some parameter experiments for structure of concentric eyewalls in TC, using the Cloud Resolving Storm Simulator (CReSS; Cloud Resolving Storm Simulator, Tsuboki and Sakakibara, 2007) which is a three-dimensional, nonhydrostatic model. And we investigate the structure of concentric eyewalls in these experiments. In our experiments, the initial wind field was axisymmetric and cyclonic vortex, which is hydrostatic and gradient wind. This wind field was based on the eq. (2) and (3) of Terwey and Montgomery (2008, hereafter TM08). The initial thermodynamic field was given by Jordan (1958; hereafter J58). The horizontal grid spacing was 2 km. The number of vertical grids was 45 and the vertical grid interval on the lowest layer was 100 m. The calculating domain had 2000 km x 2000 km x 22.5 km. The simulation time for each experiment was 500 hour. For each experiment, SST value was constant, horizontally uniformed and did not change during the simulation. We considered that structure of concentric eyewalls varies with the radial profile of the tangential wind of TC, on the basis of TM08. Therefore we conducted some parameter experiments for SST and vertical instability in the atmosphere. Because these parameters are sensitive for the maximum tangential wind of TC (Rotunno and Emanuel, 1987). We had four experiments: (1) SST = 301 K, thermodynamic field was J58, (2) SST = 302 K, thermodynamic field was J58, (3) SST = 302 K, thermodynamic field was J58 + 3 K, (4) SST = 300 K, thermodynamic field was J58 + 1 K. Here " J58 + 3 K " means that 3 K was uniformly added to the potential temperature profile of J58, and " J58 + 1 K " was the same of " J58 + 3 K " but except for the added value of 1 K. We named experiments of (1) - (4) as " CTL " , " S302 " , " ST302 " , " ST300 " , respectively.

In CTL and S302, eyewall replacements occurred on several occasions during the last 100 hours. On the other hand, in ST302, clear concentric eyewalls were formed. However, eyewall replacement did not occur over 500 hours. In ST300, concentric eyewall was not formed. In CTL and S302, the outward slope associated with height of the outer eyewall was similar to that of the inner eyewall. Moreover, the vertical wind speed in the outer eyewall was comparable with that in the inner eyewall. The other hand, in ST302, the outward slope of the outer eyewall was more gradual than that of the inner eyewall. For the vertical wind speed, it was weaker than that of the inner eyewall. These characters is also indicated in the simulated Typhoon Bolaven (2012) of Tsujino and Tsuboki (2013). Thus, we think that the occurrence of eyewall replacement is related to the similar extent of the slope between the inner and outer eyewall associated with height.

Keywords: tropical cyclone, concentric eyewall, eyewall replacement, vortex dynamics

## Mechanism of vortex movement in environmental vorticity gradient and its estimation

YAMADA, Kao<sup>1\*</sup> ; IGA, Keita<sup>1</sup>

<sup>1</sup>AORI, The University of Tokyo

Yamazaki and Itoh(2013) proposed SAM(selective absorption mechanism) as the maintenance mechanism of the blocking which is known as quasi-steady state of the atmosphere. The essence of SAM is vortex-vortex interaction and the blocking can subsist for a prolonged period by absorbing eddies of the same polarity. The movement of tropical cyclones and mid-latitude cyclones have also been investigated by vortex-vortex interaction (e.g. Fiorino and Elsberry, 1989; Oruba et al., 2012). Also, it has been indicated that the key parameters of vortex movement are the absolute vorticity gradient of the environment, the radius of vortex and its strength (e.g. DeMaria, 1985; Chan and Williams, 1987), but these researches remain at a posteriori argument of the results of the numerical simulations. In this study, we conducted numerical simulations using variety of combinations of these parameters by means of two-dimensional nondivergent barotropic model. Besides, we investigated the mechanism of the vortex movement by vortex-vortex interaction and evaluated it quantitatively.

It was found that the time-development of the vortex movement is divided into two periods with different features: the acceleration regime at the initial stage and the vortex pair translation regime with quasi-steady movement. In each regime, the vortex excites characteristic vorticity field around it and the vortex movement showed different dependence on the parameters. While the vortex slightly rotates and deforms the background field in the acceleration regime, another prolonged vortex with opposite sign appears in the eastside of the original vortex in the vortex pair translation regime.

In the acceleration regime, we evaluated the acceleration by applying directly the concept of SAM and obtained the results that the movement velocity is proportional to the product of the absolute vorticity gradient, the circulation of the vortex and the elapsed time. In the vortex pair translation regime, the velocity of the vortex movement can be evaluated by a few number of the parameters which characterize the counterrotating vortex beside, considering the mechanism of the vortex pair propagation. As a result, it is shown that the velocity is proportional to the product of the two-thirds power of the circulation of the vortex and the one third power of the planetary vorticity gradient. These estimations represent the dependence of the each-period velocity on the parameters well, and we succeeded in clarification of the physical effect on the vortex movement by the parameters and estimation of the vortex displacement.

We evaluated these parameters of the experiments for the effective beta and revealed that the difference of the influence of the planetary vorticity gradient and the relative vorticity gradient on the vortex movements results in the shear of the background flow, which has not clearly shown by previous researches.

Keywords: vortex

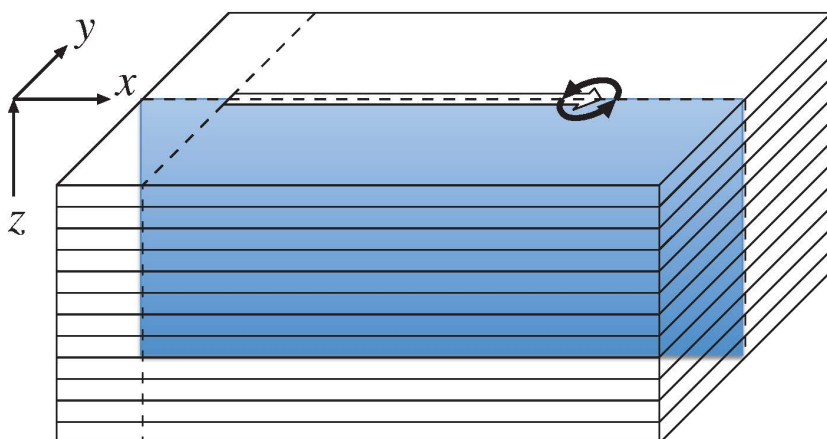
## A phase-independent expression for the energy flux associated with inertia-gravity waves

AIKI, Hidenori<sup>1\*</sup>

<sup>1</sup>Japan Agency for Marine-Earth Science and Technology

For diagnosing the effect of stationary Rossby waves on atmospheric circulation, a phase-independent expression for the wave activity flux has been developed by Takaya and Nakamura (2001) using quasigeostrophic equations. On the other hand, concerning inertia-gravity waves, a phase-expression has not been derived in previous studies. Recently we have developed a phase-independent expression for both the energy flux and the pseudo momentum flux associated with inertial-gravity waves. We have investigated the performance of the new expression using high-resolution simulations for internal waves in the ocean, such as internal gravity waves generated by a moving storm (figure) as well as tidal internal waves in JCOPE-T. The new expression for the energy flux may be used to reduce a noise associated with sampling errors in a model output, while the new expression for the pseudomomentum flux may be used for the diagnosis of mountain waves.

Keywords: inertia-gravity waves, energy flux, phase dependency



## A mechanistic model of double-diffusive intrusions

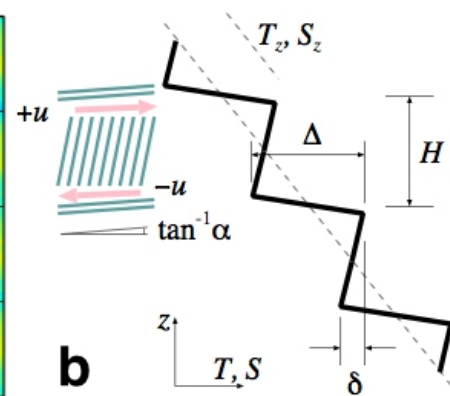
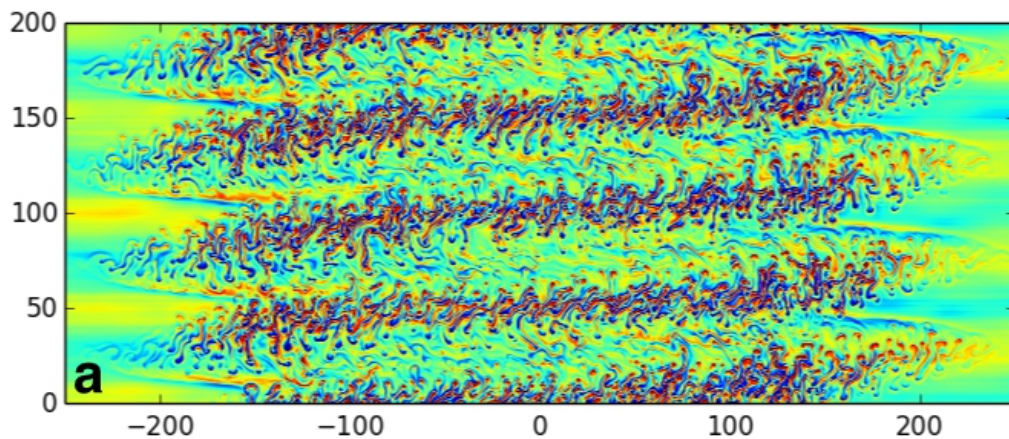
NOGUCHI, Takashi<sup>1\*</sup>

<sup>1</sup>Graduate School of Engineering, Kyoto University

Dynamical structure of double-diffusive interleaving at a density-compensating thermohaline front is investigated. Numerical simulations successfully reproduced a series of sloped intrusive motions (fig. a). It is revealed that the finger convection and its collective vertical buoyancy transport drastically changes the inner structure of the layers as well as the slope of the intrusion layers. To understand the dynamical balance of the motions in layers, a mechanistic model of intrusive layers was devised for an idealised configuration in which a unit layer repeats in vertical direction (fig. b). Transports of heat and salt by small-scale convective motions are parameterised in terms of large-scale quantities. Balances between parameterised transports yielded results qualitatively consistent with that of the numerical simulations.

Acknowledgements: This work was supported by JSPS Grant-in-Aid for Young Scientists B 23740354.

Keywords: double-diffusive convection, lateral mixing



## Low-frequency internal waves in Shiozu Bay, Lake Biwa: A numerical approach

AUGER, Guillaume<sup>1\*</sup> ; NAGAI, Takeyoshi<sup>2</sup> ; YAMAZAKI, Hidekatsu<sup>2</sup>

<sup>1</sup>Department of Civil Engineering, Ritsumeikan, <sup>2</sup>Department of Ocean Science, TUMSAT

In this study, we present results from the three-dimensional unstructured numerical simulator SUNTANS, used to understand the dynamics of the low-frequency internal wave field inside Shiozu Bay, a bay in the Northern part of Lake Biwa. Initial conditions for a fine-scale grid were generated in using a coarse grid with measured heat fluxes and wind stress. After being compared against observational data, the simulation reproduced consistently the low-frequency internal wave field, (similar frequencies and waves features). Based on the analysis of integrated potential energy and integrated dissipated energy time series, this study shows that the low-frequency internal wave field that enters Shiozu Bay does not either completely dissipate or break. Moreover isotherm elevation associated to the internal the first horizontal mode and first vertical mode Kelvin wave highlights the cyclonic rotation pattern, which is characteristic of the Kelvin wave, within the bay. This result shows that the part of the Kelvin wave entering the bay goes in and out. Moreover the dynamic of the internal wave field within the bay displays an peculiar process at the narrowing of the bay. At the contraction of the bay, the flow speeds up and deep isotherms deepen further. These two processes generated turbulence by shear and strain; according to the turbulence model (Mellor and Yamada, 1982) turbulent kinetic dissipation rate reached  $10^{-6} \text{ W kg}^{-1}$ , occurring during the trough phase of the internal wave field. Additionally the occurrence of these enhanced turbulent events appears to depend on the amount of energy detained by the low frequency internal wave. When the internal wave field was energized by the wind the turbulent events were enhanced. Such events could modify the long-term distribution of material in the lake.

Keywords: wind forcing, internal waves, contraction, strain

## Anomalous wave dispersion of distant tsunamis in a coupled system between the self-gravitating elastic Earth and ocean

WATADA, Shingo<sup>1\*</sup>

<sup>1</sup>Earthquake Research Institute, University of Tokyo

Traveltime delay and waveform dispersion of distant tsunamis that propagated over the Pacific after the 2010 Chilean and 2011 Tohoku-Oki earthquake can be understood as a propagating wave in a unified gravitationally and elastically coupled system between the solid Earth and ocean.

Keywords: Tsunami propagation delay, Tsunami phase velocity measurements, Tsunami waveform dispersion, Tsunami initial phase with reversed polarity, Tsunami precursor, DART tsunami records from the 2010 Tohoku?Oki earthquake and

## On the vigor of mantle convection and stagnant lid formation in super-Earths

MIYAGOSHI, Takehiro<sup>1\*</sup>; KAMEYAMA, Masanori<sup>2</sup>; OGAWA, Masaki<sup>3</sup>

<sup>1</sup>JAMSTEC, <sup>2</sup>Ehime University, <sup>3</sup>University of Tokyo

Super-Earths are extra-solar terrestrial planets which have large sizes and masses (up to about ten times the Earth's mass). Understanding mantle convection in super-Earths is a key to clarifying their evolution, surface environment, and habitability. In large super-Earths, the mantle depth far exceeds the thermal scale height, and adiabatic compression strongly influences super-Earths' mantle convection in contrast to the Earth's one. In this paper, we present numerical models of mantle convection in super-Earths with high compressibility, high Rayleigh number, temperature-dependent viscosity and depth-dependent thermal expansivity.

Thermal convection of compressible infinite Prandtl number fluid is solved in a rectangular box under anelastic approximation by the ACuTEMAN (Kameyama et al. 2005). The model of the super-Earths includes depth-dependent thermal expansivity and density, as well as a strong temperature-dependence of viscosity. We assume the mass of the planet is ten times the Earth's. The Rayleigh number defined with the viscosity at the core-mantle boundary (CMB)  $Ra$  is  $1E10$ . A viscosity contrast  $r$  up to  $1E7$  arises between the CMB and the surface owing to the temperature-dependence of viscosity. The employed grid number is 1024 (horizontal) and 256 (vertical).

We identified the stagnant lid regime in the model of super-Earths. When the viscosity contrast  $r$  is larger than about  $1E6$ , a stagnant lid of highly viscous fluid is formed along the surface. The lid hardly moves and is not involved in the convection, as has been observed earlier for the Boussinesq model of the Earth's mantle convection (Kameyama and Ogawa, 2000). The lithosphere is as thick as about thirty percent of the depth of the whole mantle, and the Nusselt number is about three at  $r=1E7$  and  $Ra = 1E10$ . This value is comparable to that of the Earth's model at the same  $r$  but at much lower  $Ra$  of  $6E6$  (Kameyama and Ogawa, 2000). The lithosphere is much thicker than has been expected earlier for super-Earths (e.g., Valencia et al. 2007), and the thick lithosphere is likely to affect the possibility of plate tectonics at the surface of super-Earths. The strong effect of adiabatic compression also affects the dynamics of hot plumes that ascend from the CMB when the temperature-dependence of the viscosity is strong: At  $r > \sim 1E3$ , hot plumes from the CMB are strongly suppressed. They do not ascend to the surface of the planet. The overall pattern of convective circulation in the mantle is, therefore, dominated by the cold plumes that descend from the lithosphere to the CMB. The low efficiency of heat transport by the mild convection would strongly affect the evolution history of super-Earths, and is likely to weaken the core convection, and thus, the magnetic field of super-Earths.

Keywords: super-Earths, mantle convection

## Heater size effect on generation of thermal plumes

KUMAGAI, Ichiro<sup>1\*</sup> ; YAMAGISHI, Yasuko<sup>2</sup>

<sup>1</sup>Meisei University, <sup>2</sup>IFREE, JAMSTEC

Mantle plumes from the CMB experience a filtering effect by the endothermic phase change at the 660-km phase transition. Fluid dynamics predicts that the hot mantle plumes stagnate at and locally heat the upper-lower mantle boundary, which causes generation of the secondary plumes in the upper mantle, and hence hotspots volcanic activities on the surface. To understand the effects of heater size on the plumes generation, we have experimentally investigated the behaviors of thermally buoyant plumes generated from a localized heat source (circular plate heater) using quantitative visualization techniques of temperature (TLC) and velocity (PIV) fields. Scaling laws for their ascent velocity and spacing of the plumes are experimentally determined. We also estimate the onset time of the secondary plumes in the upper mantle which depends on local characteristics of the thermal boundary layer developing at the upper-lower mantle boundary.

Keywords: plume, mantle, fluid dynamics, experiment

## Waves and linear stability of magnetoconvection in a rotating cylindrical annulus

HORI, Kumiko<sup>1\*</sup> ; TAKEHIRO, Shin-ichi<sup>2</sup> ; SHIMIZU, Hisayoshi<sup>1</sup>

<sup>1</sup>Earthquake Research Institute, University of Tokyo, <sup>2</sup>Research Institute for Mathematical Sciences, Kyoto University

Magnetohydrodynamic waves in a rapidly rotating planetary core can cause the magnetic secular variation. To strengthen our understanding of the physical basis of such waves, we revisit the linear stability analyses of thermal convection in a quasi-geostrophic rotating cylindrical annulus with an applied toroidal magnetic field, and we extend the investigation of the oscillatory modes to a broader range of the parameters. Particular attention is paid to influence of thermal boundary conditions, either fixed temperature or heat-flux conditions.

While the non-dissipative approximation yields a slow wave propagating retrograde (westward), termed as a Magnetic-Coriolis/Magnetic-Coriolis-Archimedes (MC/MAC) Rossby wave, dissipative effects produce a variety of waves. When magnetic diffusion is much stronger than thermal diffusion, this can cause a very slow wave propagating prograde (eastward). Retrograde-travelling slow waves appear when magnetic diffusion is weaker. Emergence of the slow modes allows convection to occur at lower critical Rayleigh numbers than in the nonmagnetic case. When the magnetic diffusion is strong, the onset of the convection occurs with the prograde-propagating slow wave, whereas when it is weak, a slow MC mode conducts the critical convection.

Fixed heat-flux boundary conditions have profound effects on the marginal curves, which monotonically increase with the horizontal wavenumber, and lead to larger length scales at the onset of the convection, provided there is sufficient field strength that the Lorentz force is balanced with the Coriolis force. The effect, however, becomes less clear as the magnetic diffusion is weakened and various magnetohydrodynamic waves emerge.

## Investigation of cell patterns on a rotating convection by ultrasonic velocity profile measurements

FUJITA, Kodai<sup>1\*</sup> ; TASAKA, Yuji<sup>1</sup> ; MURAI, Yuichi<sup>1</sup> ; OISHI, Yoshihiko<sup>1</sup> ; YANAGISAWA, Takatoshi<sup>2</sup>

<sup>1</sup>Hokkaido University, <sup>2</sup>IFREE JAMSTEC

Rayleigh-Benard convection is the well-known topic as fundamental system in fluid dynamics. In particular, the effect of rotating field on the convection is one of essential piece for geophysics. The influence of centrifugal force and Coriolis force on convection pattern formation was experimentally showed by Rossby (1969). The flow structure of Rayleigh-Benard convection in a rotating field is described by Rayleigh number (Ra), Taylor number (Ta) and Prandtl number (Pr). Especially, it is important to study the behavior of low Pr fluid like liquid metals, because this knowledge helps to understand the dynamics of metallic cores in planets. In low Pr fluids, the flow regimes dramatically changes in comparison with ordinal fluid with  $Pr > 1$ . For example, Rayleigh-Benard convections in a liquid metal layer easily take transition to turbulent state. Generally, adding rotating field stabilizes the flow. On the other hand, flows of low Pr fluids with background rotation are expected to become oscillatory and irregular motion near the marginal stability conditions. These characteristics of low Pr fluids, however, have not been studied experimentally so much, because it is impossible to capture the convection patterns of liquid metal flows optically. To solve this problem, the authors adopt Ultrasonic Velocity Profile (UVP) method to visualize convective flow of liquid metal in a rotating field. As the data set of UVP measurement is one-dimensional velocity distribution, it is difficult to guess flow fields of convection from only a result of UVP without any criterion of translation. In this study, as preparations for liquid metal experiments, we performed two different visualizations using optics and ultrasound on ordinal transparent fluid, water ( $Pr = 7$ ), to understand flow field from spatio-temporal velocity distribution obtained by UVP. Optical visualization provides path line images for the comparison. In addition, we purpose to take the knowledge about spatio-temporal velocity distribution of high Pr contrasted with low Pr.

Experiments were performed on a rotating table. The vessel of fluid layer has a square geometry, which aspect ratio is seven. The bottom of fluid layer was heated by electrical heating and the upper surface was cooled by circulating water through flow channel made of glass plate. Optical visualization images were obtained from a horizontal section of the fluid layer. An ultrasonic transducer for UVP measurement was mounted horizontally on the side wall of fluid layer.

The path line showed many small round convective cells in the fluid layer, and it represented that the size of cells become smaller as Ta takes larger. In addition, the size of cell and cell motions were also detected by spatio-temporal velocity distributions acquired by UVP. For example, cells moved in certain direction and passed over measurement line of transducer. Staying time of cell on the line was observed and means speed of cells moving. As Ta gets larger, it was found that the speed of each cell motion became slower. The cell diameter was calculated from velocity data. When cells stay next to each other, there is 0 mm/s on cells boundaries in spatial velocity distribution at the time. We defined distances between neighboring cells on the spatial line respectively as scales of cell size. Then we extracted all distances from spatio-temporal distribution and calculated the expected value of these. The expected value represents dominant cell diameter. We confirmed that the cell size on the distribution roughly corresponds to that on the path line. Thereby we obtained information of convective cell from only UVP data.

Keywords: Rayleigh Benard convection, Rotating field, Flow pattern

## Roll convection in a liquid metal layer subject to a horizontal magnetic field

TASAKA, Yuji<sup>1\*</sup> ; IGAKI, Kazuto<sup>1</sup> ; YANAGISAWA, Takatoshi<sup>2</sup> ; ECKERT, Sven<sup>3</sup> ; MURAI, Yuichi<sup>1</sup>

<sup>1</sup>Faculty of Engineering, Hokkaido University, <sup>2</sup>JAMSTEC, <sup>3</sup>Helmholtz center at Dresden-Rossendorf

Recent investigations using ultrasonic velocity profiling (UVP) on Rayleigh-Benard convection in a liquid metal layer under horizontal magnetic field gave good understanding for typical temperature fluctuations shown in previous studies (Yanagisawa, et al., 2013). For example, regime transition against variations of Rayleigh number (Ra) and Chandrasekhar number (Q), variation of the roll number and spontaneous, random flow reversal that consists of spontaneous transition between two modes having different number of rolls, mainly  $N = 4$  and  $5$ . This flow reversal may be due to non-integer number of stable wave number in corresponding conditions of Ra and Q. The rolls can take only integer number even though the stable wave number determined by flow instability is, for example,  $N = 4.3$ . In this case the dominant condition is  $N = 4$ , and it is sometime modified into  $N = 5$  due to external noise. However,  $N = 5$  is not stable, and thus Skewed varicose instability occurs to restore  $N$  into  $4$ . Time average of instantaneous  $N$  may correspond to stable wave number for the corresponding conditions.

This study aims to widen the flow regimes into larger Ra and larger Q by one order to clarify the influence of strong magnetic field: Past studies predict that the strong magnetic field greatly modifies the critical Rayleigh number at the onset of the convection. Experiments were done in Helmholtz center at Dresden-Rossendorf (HZDR) to utilize strong magnetic field generator that can provide quasi uniform magnetic field with 30 mT in the intensity. The test fluid layer is almost same with our previous study (Yanagisawa, et al., 2013) and its main aspects are, 5 in aspect ratio, 40 mm in height and sandwiched between copper plates for cooling at top and heating at bottom. The obtained regime diagram shows that the fraction rule on Ra/Q determining the regimes is still almost valid in the widen region of Ra and Q. But the number of rolls is slightly modified from expectations by the rule. Also we observed "regular" flow reversals instead of random one. This may be due to stable number of rolls larger than  $N = 4.5$  and aspect ratio of the vessel, 5. The dominant roll number also depends on the side boundary of the vessel. Velocity profiles parallel to the roll axes clarified three dimensional motion during the regular flow reversals.

Keywords: Rayleigh-Benard convection, Liquid metal, Magnetic field, Convection pattern

## Flow reversals in liquid metal convection by the skewed-varicose instability

YANAGISAWA, Takatoshi<sup>1\*</sup> ; SAKURABA, Ataru<sup>2</sup> ; HAMANO, Yozo<sup>1</sup>

<sup>1</sup>IFREE, JAMSTEC, <sup>2</sup>School of Science, Univ. Tokyo

The natures of turbulence and large-scale flow pattern in the outer core are controlled by the magnetic field. It is important to know the basic behavior of flow in relation to the magnetic field, for understanding the flow patterns observed in real Earth and core dynamo simulations. By recent laboratory experiments of Rayleigh-Benard convection with liquid gallium, a regime diagram of convection patterns was established under various intensities of a uniform horizontal magnetic field for a wide square geometry (Yanagisawa et al. 2013, PRE). Five flow regimes are recognized; (I) fluctuating large-scale pattern without roll, (II) weakly constrained roll with fluctuations, (III) continuous oscillation of roll, (IV) repetition of roll number transitions with random reversals of the flow direction, and (V) steady 2-D rolls. In these, regime (IV) with flow reversals is the most interesting behavior. Flow reversals have been observed so far in narrow vessels with small aspect ratio, and the proposed processes for reversals are reorientation and cessation. Experiments with liquid metal under horizontal magnetic field suggest the existence of new type of reversal, via the skewed-varicose instability.

We performed numerical simulations of magnetoconvection in a same setting as the experiment with no-slip velocity boundary conditions. Both the Prandtl number and magnetic Prandtl number of the working fluid are set small to simulate liquid metals. Our numerical result successfully reproduced all regimes that observed in the experiments. The process of flow reversal is illuminated by the simulation. Axis of roll is skewed with a roll shrinking, and the number of rolls is reduced. In case the reduced roll number structure is not fit the vessel, new small circulation grows to a roll again, and then reversed flow state is established. The process repeats with irregular time interval. It works in 3-dimensional geometry, and should play important role in various flow systems.

Keywords: thermal convection, liquid metal, flow reversal

## Spectrum of internal waves in bounded domains of the Atmosphere and the Ocean

GINIATOULLINE, Andrei<sup>1\*</sup>

<sup>1</sup>Department of Mathematics, Los Andes University, Bogota, Colombia, South America

We consider the spectral properties of internal waves for three-dimensional compressible rotating exponentially stratified fluid. This model describes the flows in the Atmosphere and the Ocean which include simultaneously the rotation of the Earth over the vertical axis, and the non-homogeneous initial stratification of density caused by the gravitational force. We obtain theoretical results for the spectrum of the resulting internal waves in terms of its structure, localization, and its possible usage in computational algorithms. The applications of the spectral properties of such internal waves can be found, in particular, in the models of the resonance effect. We consider both the general case of bounded domains, and the explicit results of some particular domains, such as cubes and cylinders.

Keywords: computational fluid dynamics, compressible fluid, rotating stratified fluid, essential spectrum, internal waves, fluid dynamics of the Atmosphere and the Ocean